JMEPEG (2006) 15:299-305
DOI: 10.1361/105994906X108701

1059-9495/$19.00

Investigation of Residual Stress by the Indentation Method with the Flat Cylindrical Indenter

B.X. Xu, B. Zhao, and Z.F. Yue

(Submitted July 25, 2005; in revised form September 11, 2005)

Experiments and numerical simulations have been carried out to study residual stress of copper specimens by the indentation method with a flat cylindrical indenter. Copper specimens were annealed at different temperatures for 35 min to obtain different residual stress levels. The experiments carried out on these specimens demonstrated the influence of residual stress on indentation behavior. The influence of annealing temperature on the elastic-plastic transition region is quite obvious. A method has been presented to determine material properties, such as elastic modulus and Poisson ratio. This method can also be applied to determine residual stress with the assumption of knowing the yield stress in advance. The advantage of this method is that it can avoid calculating the contact area. In the finite element modeling (FEM), residual stresses on copper specimens are simulated by preapplying stresses. The influence of residual stress on the indentation load-depth curves has been studied by FEM. There is good agreement between experimental and FEM numerical results. A numerical method has also been presented to determine residual stress. In addition, Mises stress and plastic distribution ahead of the indenter have also been studied to help us further understand the influence of residual stress.

Keywords anneal, elastic-plasticity, finite element analysis, indentation experiment, residual stress

1. Introduction

As a localized testing method, indentation testing has been widely used to determine material mechanical properties, such as elastic modulus (Ref 1–3), yield strength (Ref 4, 5), creep material parameters (Ref 6–8), hardness (Ref 9, 10), strain-hardening modulus (Ref 11, 12), and fracture toughness (Ref 13, 14). But most indentation research models are based on the assumption that there is no residual stress. The experiment carried out by Sines and Carlson (Ref 15) showed that the measured hardness decreases if there is tensile residual stress and increases if there is compressive residual stress. These results show that residual stress can be determined by the indentation method.

In past decades, many researchers have tried to determine residual stress with the indentation method (Ref 16-22). Tsui et al. (Ref 16) studied the influence of residual stress on hardness and elastic modulus with Berkovich diamond indenters. Their results showed that the dependence of hardness is similar to the results of Sines and Carlson, while for the elastic modulus, the discrepancy is as much as ~10%. However, subsequent finite element analysis revealed that the dependence of hardness was not real but rather an experimental artifact that was caused by an influence of the stress on the geometry of up-piling around the hardness indentation (Ref 17). Inspired by Tsui, Suresh and Giannakopoulos suggested a method that was based on the difference in contact area of stressed and unstressed materials at the same depth with Berkovich diamond indenters (Ref 18). In fact, the influence of residual stress on the contact area is relatively small. It is not clear that the method can be practically applied except that residual stress is near yield stress, and the pile-up is obvious in materials. This method has not yet been verified by experiment.

Motivated by the results obtained with Berkovich diamond indenters, Taljat and Pharr suggested that much larger effects from residual stress can be measured by using the indentation with blunt, spherical indenters (Ref 19). Their finite element analysis results showed that the indentation load-depth curves in the transition regimen between elastic contacts at the small indentation depth and fully developed plastic contact at lager loads were affected by residual stress. To examine the finite element results. Swadener et al. (Ref 19) performed spherical indentation experiments on a polished disk of commercial aluminum alloy, to which compressive or tensile biaxial stress had been pre-applied to the specimen surface. They found that indentation load-depth curves shifted to the larger indentation depth when the applied biaxial stress is tensile stress, while compressive stress had the opposite effect. On the basis of these experimental results, Swadener et al. (Ref 19) reported two methods for measuring residual stresses using spherical indenters. The basic idea of the first method relies on the expression:

$$\frac{\sigma_R}{\sigma_y} = 1 - \frac{4}{3\Psi\pi}\left(\frac{E_e a}{R\sigma_y}\right)_o \qquad \text{(Eq 1)}$$

where σ_R, σ_y, E_e, a, R, and Ψ are residual stress, yield stress, effective elastic modulus of equation of Oliver (Ref 2), contact radius, the radius of spherical indenters and constrain factor, respectively. The value of $E_e a/R\sigma_y$ can be determined by extrapolating from a plot of h_f/h_{max} (the ratio of maximum indentation depth to residual indentation depth) versus $E_e a/R\sigma_y$, and parameter a can also be known from the onset of yielding.

B.X. Xu, **B. Zhao**, and **Z.F. Yue**, Department of Engineering Mechanics, Northwestern Polytechnical University, Xi'an 710072, People's Republic of China. Contact e-mail: zfyue@nwpu.edu.cn.

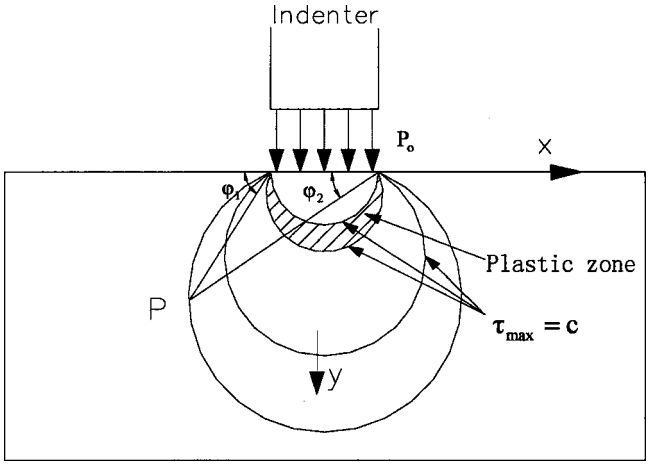

Fig. 1 Simplified model for a flat cylindrical indenter indented on a bulk material

However, this method has the disadvantage of contact area calculation, which is difficult because of the influence of uppile around the indenters. The second method is based on the relationship between $E_e a/R\sigma_y$ and $\Psi\sigma_f$ that was established by experiments in a reference specimen with a known state of stress. However, for the mean pressures P_m, there is only a relatively small discrepancy when $E_e a/R\sigma_y$ is the same, although residual stress has changed greatly, especially when residual stress is compressive stress. In addition, there is no fixed relationship.

On the basis of these experimental and finite element results, which were measures of residual stress by indentation methods with sharp or spherical indenters, it was suggested that residual stress can be more easily measured with flat cylindrical indenters and that the accuracy is higher than that measured with other geometric shape indenters. Experiment and finite element simulation were done to confirm these results in the subsequence. Two methods are put forward to measure residual stress with flat cylindrical indenters: The first method requires the yield stress of materials be known in advance; compared with other methods, this method avoids calculating the contact area. In addition, the elastic modulus and Poisson's ratio can also be obtained. The second method requires that a series of the indentation experiment be done to establish the relationship between residual stress and indentation load.

2. Simplified Theoretical Model to Explain the Influence of Residual Stress on Hardness

The model is shown in Fig. 1. The indentation load is P_o. The stress state of point P in Fig. 1 is:

$$\sigma_x = -\frac{P_o}{2\pi}[2(\varphi_1 - \varphi_2) + \sin 2\varphi_1 - 2\sin 2\varphi_2] \quad \text{(Eq 2)}$$

$$\sigma_y = -\frac{P_o}{2\pi}[2(\varphi_1 - \varphi_2) - \sin 2\varphi_1 - 2\sin 2\varphi_2] \quad \text{(Eq 3)}$$

$$\tau_{xy} = \frac{P_o}{2\pi}[\cos 2\varphi_1 - \cos 2\varphi_2] \quad \text{(Eq 4)}$$

The maximum shear stress τ_{max} of point P is:

$$\tau_{max} = \pm\sqrt{\left(\frac{\sigma_x - \sigma_y}{2}\right)^2 + \tau_{xy}^2} \quad \text{(Eq 5)}$$

and further,

$$\tau_{max} = \pm\frac{P_o}{\pi}\sin(\varphi_1 - \varphi_2) \quad \text{(Eq 6)}$$

It is obvious from Eq 6 that plastic deformation occurs first at:

$$\varphi_1 - \varphi_2 = \frac{\pi}{2}.$$

To simplify analysis, it is assumed that residual stress only exists in the radial direction, i.e., $\sigma_{yR} = 0$ and $\sigma_{xR} \neq 0$. Using the same method, the maximum shear stress τ'_{max} can also be obtained when there is residual stress in the radial direction.

$$\tau'_{max} = \sqrt{\frac{P_o^2}{\pi}\sin^2(\varphi_1 - \varphi_2) - \frac{P_o}{\pi}\sin(\varphi_1 - \varphi_2)\cos(\varphi_1 + \varphi_2)\sigma_{xR} + \frac{\sigma_{xR}^2}{4}} \quad \text{(Eq 7)}$$

In Eq 7, when residual stress σ_{xR} is tensile stress, the maximum shear stress τ'_{max} is greater than τ_{max}. So the plastic deformation occurs earlier than without residual stress, and it results in a decrease in the hardness, while compressive stress has the opposite effect. Those results are also in agreement with results in Ref 15. In addition, for the plane stress, the conclusion also is that residual stress does not have affect hardness for $\sigma_{xR} = \sigma_{yR}$.

3. Determining Residual Stress in the Elastic Region

If the deformation is in the elastic region, Hayes's relationship can be used to obtain the indentation load-depth as (Ref 23):

$$\frac{P}{h} = \frac{2Ea}{1-\nu}\kappa(a/t,\nu) \quad \text{(Eq 8)}$$

where p, h, E, a, t, and ν are indentation load, indentation depth, elastic modulus of the indented material, radius of indenters, maximum depth of the elastic deformation (which can be measured from the indentation depth after unloading), and Poisson ratio. $\kappa(a/t,\nu)$ is a correction factor. If two indenters with different size are applied, the following equation can be derived:

$$\frac{\left(\frac{P}{h}\right)_1}{\left(\frac{P}{h}\right)_2} = \frac{a_1}{a_2}\frac{\kappa(a_1/t,\nu)}{\kappa(a_2/t,\nu)} \quad \text{(Eq 9)}$$

From Eq 9, it is easy to derive the Poisson ratio, ν. With the help of Eq 8, the elastic modulus can also be obtained.

As the indentation load increases, the yield criterion for the material is reached, after yielding has initiated, Tabor's relation can be used to relate the relationship between applied indentation stress P_m ($= P_0/\pi r^2$, r is the radius of indenters) and the effective flow stress σ_f through Eq 10 (Ref 24),

$$P_m = C\sigma_f \quad \text{(Eq 10)}$$

where C is a constraint factor. For the Tresca yield condition without friction, Shield found that the exact solution of the constraint factor C for the axisymmetric flat cylindrical indenter is 2.571 for the edge of the indenter (Ref 25).

When there is a residual stress σ_R in the materials, according to Ref 19 and 20, Eq 10 can be written as follows as long as yielding initiates below the surface:

$$P_m = 2.571(\sigma_y - \sigma_R) \quad \text{(Eq 11)}$$

where residual stress is positive for tension and negative for compressive. The applied indentation stress P_m can be given as:

$$P_m = \frac{P}{\pi a^2} = \frac{2Et}{\pi(1-v)a}\kappa(a/t,v) \quad \text{(Eq 12)}$$

So residual stress can be obtained by Eq 11 and 12, that is to say, residual stress can be given as the following equation:

$$\frac{\sigma_R}{\sigma_y} = 1 - \frac{0.778}{\pi}\left(\frac{Et\kappa(a/t,v)}{a(1-v)\sigma_y}\right) \quad \text{(Eq 13)}$$

Now, elastic modulus, Poisson ratio, and residual stress are obtained step by step. It is obvious that this method avoids the discrepancy that is caused by calculating elastic modulus from the unloading curves, and precision is also improved.

4. Experimental Details

The material chosen for our studies was copper with 0.0262% Zn, 0.0145% P, 0.003% Pb, and 0.1266% Fe. Copper specimens were annealed at two different temperatures, 250 and 100 °C, for 35 min to relieve residual stress at two different levels. The material of the flat cylindrical indenters was alloy steel.

The indentation experiment was performed using a conventional INSTRON 8871 (London, UK) tensile machine, which was designed to couple a flat cylindrical indenter with radius 0.75 mm. The indentation load-depth (crosshead displacement) can be continuously recorded throughout the experiment. In the experiment, the machine crosshead was drawn at a constant velocity 0.025 mm/s in the loading stage and 0.05 mm/s in the unloading stage for each specimen. The detail fixture is shown in Fig. 2.

5. Experimental Results

It is believed that there are different residual stresses in the two specimens that were relieved partially at two different anneal temperatures, respectively. The indentation load-depth curves for the specimens annealed at different temperatures were first obtained at room temperature to study the influence of residual stress. The experimental results are shown in Fig. 3.

From Fig. 3, in the initial section, the curves are not linear mainly due to the influence of surface roughness. The unloading-depth curve is approximately linear in the unloading stage, which makes it easier to obtain the elastic modulus than other geometric shape indenters if the formula is used to measure the elastic modulus explored in Ref 2. In addition, this approximately linear relationship has also shown that contact between the surface and the indenter is nearly unaffected by the up-pile around the flat cylindrical indenter.

It can be seen that the influences of specimens' annealed temperature on the loading curves are obvious, especially in the elastic-plastic transition stage. The main discrepancy in the "elastic-plastic" transition regimen is shown in Fig. 3(b). This figure shows that the influence of residual stress on the indentation load-depth mainly occurs at the "elastic-plastic" transition regimen. Compared with the results obtained with spherical indenters (Ref 19), this influence is more obvious. In addition, when the indentation is in the elastic-plastic transition region, residual stress is also been estimated easily. This method is similar to the method for determining the yield stress of the material shown in Ref 12.

6. Finite Element Analysis

6.1 Uniaxial Tensile Experiment and Material Parameters

The uniaxial tensile experiment was carried out to obtain the stress-strain relationship at room temperature of a copper specimen annealed at 150 °C for 35 min. The stress-strain curve is shown in Fig. 4. From Fig. 4, the elastic modulus $E = 115.9$ GPa can be obtained. After the copper specimen was obtained at 51.6 MPa, a small amount of work hardening is observed, the work hardening exponent of which is ~0.54. Later, the stress reaches a relative constant value of 231.6 MPa. This property indicates that the copper specimen behaves very similarly to the elastic-perfectly plastic solid with a flow stress of 231.6 MPa.

6.2 FEM Model

An asixsymmetric finite element model was used to calculate the deformation development around the flat cylindrical indenter. The indenter can be assumed to be rigid, and friction

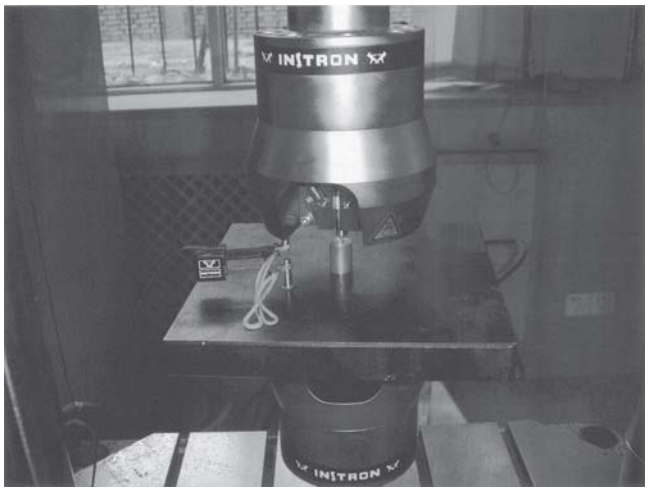

Fig. 2 Fixture for the indentation experiment with a flat cylindrical indenter

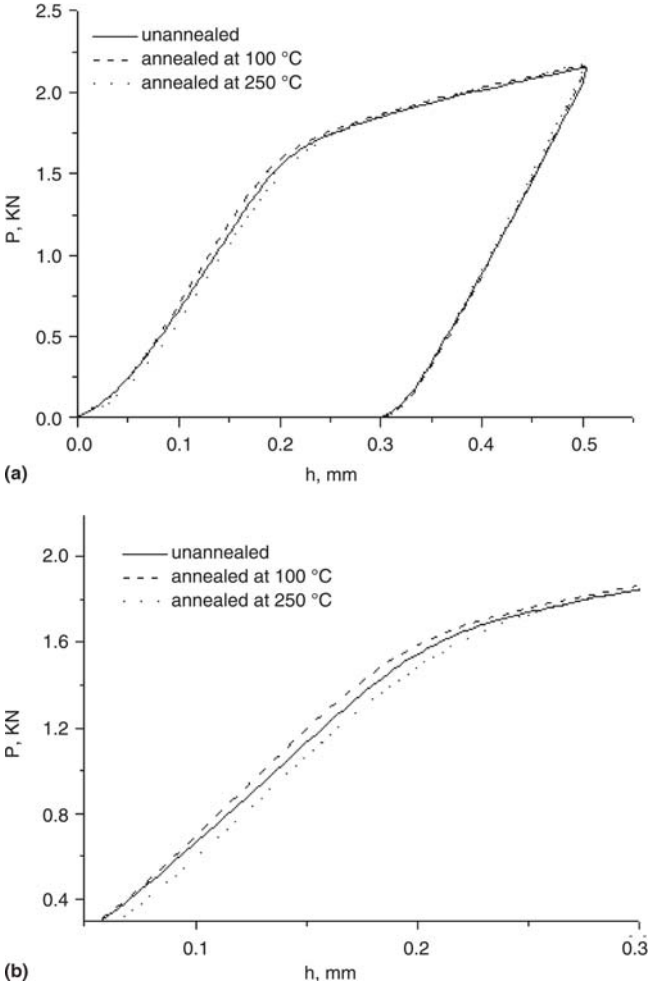

Fig. 3 Indentation load-depth curves were obtained from copper specimens annealed at two temperatures for 35 min: (a) loading and unloading curves; (b) influence on the elastic-plastic transition region in the loading stage

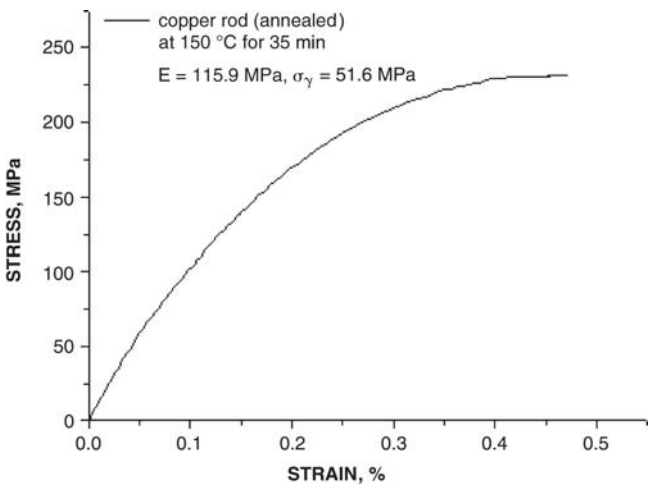

Fig. 4 Uniaxial tensile stress-strain relationship for the copper specimen annealed at 150 °C for 35 min; this curve has been put into the finite-element simulation as a material model.

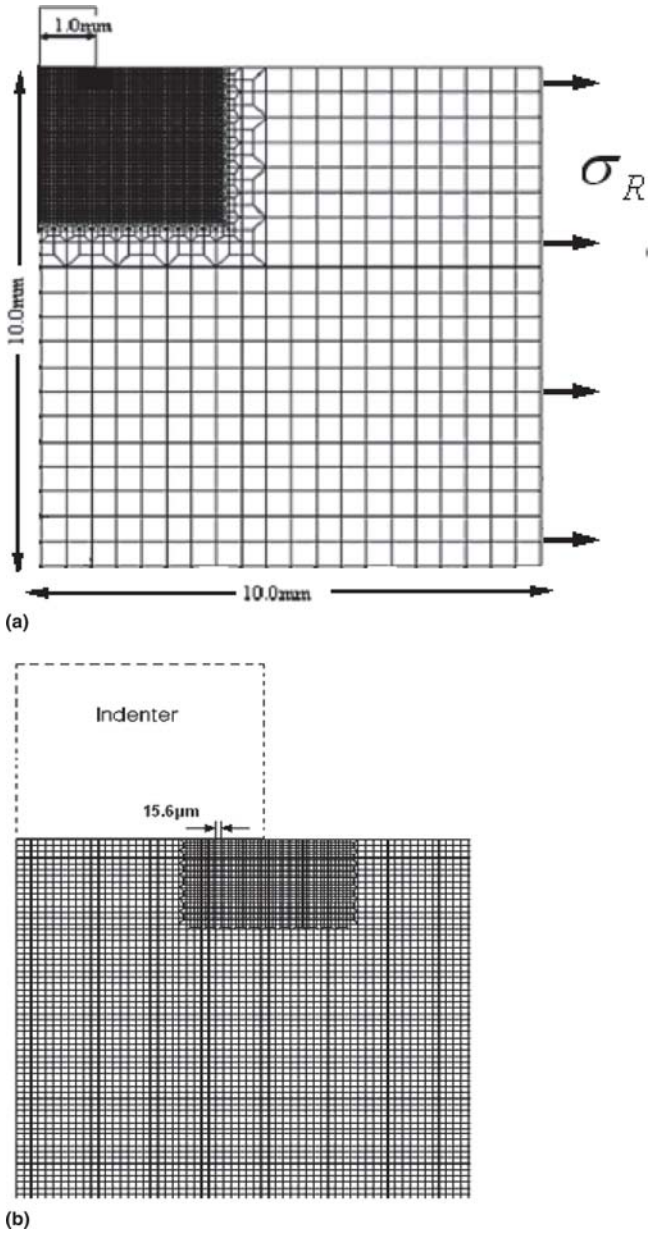

Fig. 5 Axisymmetric finite-element mesh: (a) overall finite element mesh and boundary conditions; (b) fine portion of finite element mesh in contact region near the flat cylindrical indenter, especially at the edge of the indenter

between the surface of the flat cylindrical indenter and the indented material are also neglected according to experimental and numerical analysis results (Ref 26, 27). So the contact calculation can be avoided by loading the uniform indentation stress and keeping the same indentation depth when the surface area is in contact with the indenter, which can be realized by a technology of MPC cards (Ref 28). The finite element mesh and boundary conditions are shown in Fig. 5(a) and (b). In finite element analysis, in the radial-surface of the cylinder, uniform stress (residual stress), −200, −150, −100, −50, 0, 50, 100, 150, and 200 MPa, was preapplied to simulate residual stress of copper specimens, where the minus sign denotes compression and the positive sign denotes tension. The simulation was completed in the finite element analysis software ABAQUS (Ref 28).

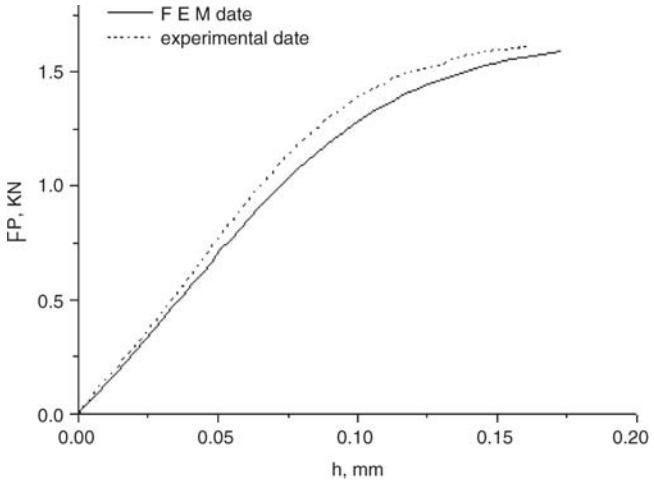

Fig. 6 Curves obtained from the indentation experiment and numerical simulation. The experimental curve is obtained from the copper specimen annealed at 150 °C for 35 min. The finite-element result is obtained without preapplied stress, and the material properties used in the numerical simulation are shown in the figure.

7. FEM Results

7.1 Comparison of FEM Numerical and Experimental Results

To confirm the finite element analysis model, a finite element simulation was first studied to obtain indentation load-depth curve for a direct comparison with results of the actual indentation experiment in the copper specimen. For the finite element model, the radius of the indenter is 0.75 mm, and the experimental dates are obtained from the annealed copper specimen at 150 °C for 35 min. The experiment and simulation were all loaded by displacement. The results are shown in Fig. 6. It can be seen that agreement is good. The main discrepancy also occurs at the elastic-plastic transition region.

7.2 Influence of Residual Stress (Preapplied Stress) on Indentation Load-Indentation Depth Curves

Figure 7 shows the influence of residual stress on indentation load-indentation depth. It is shown that the indentation depth increases with increasing of tensile residual stress, while the indentation depth decreases with increasing of compressive residual stress. This inversely proportional relationship was also in agreement with the relationship between hardness and residual stress. It is shown that residual stress can be determined from the relationship between indentation stress and residual stress under a certain indentation depth (Fig. 7). The detailed process can refer to the method to estimate the yield strength from the indentation depth-indentation stress curve, shown in Ref 12.

7.3 Influence of Residual Stress (Preapplied Stress) on Mises Stress Distribution

Figure 8 shows that the influence of residual stress on Mises stress distribution ahead of the indenter. From Fig. 8(b), it is shown that another low-stress region occurs ahead of the indenter when the residual stress is tensile stress, and it moves down with decreasing residual stress. The reason is that the compressive stress induced by humps near the indentation interacts with residual tensile stress. As a comparison, the paper has also given Mises stress distribution ahead of the indenter without residual stress, as shown in Fig. 8(c).

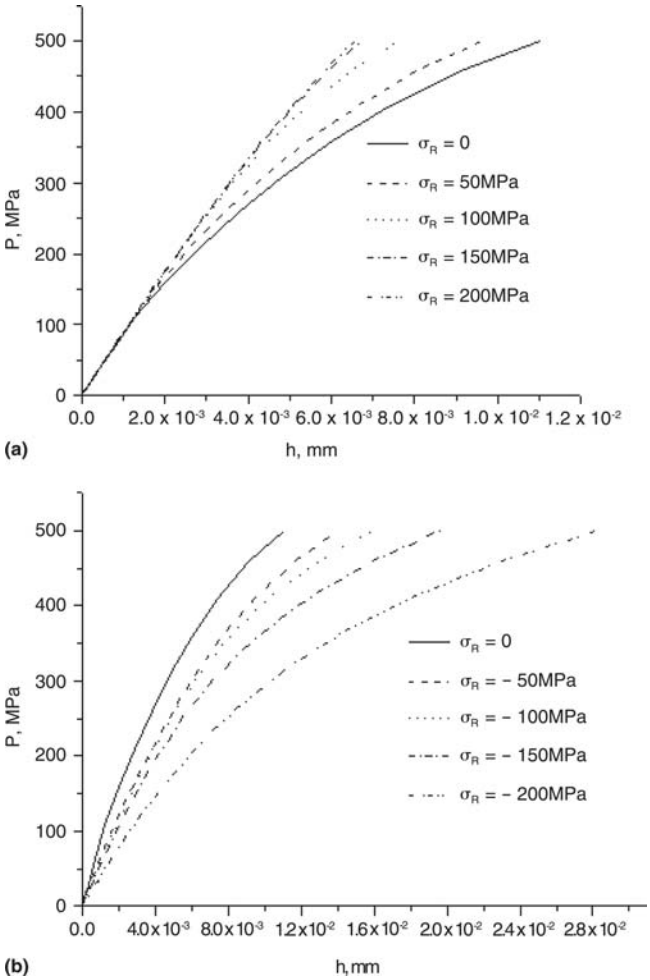

Fig. 7 Indentation load-indentation depth curves under different applied stresses: (a) applied stress is tensile stress; (b) applied stress is compressive stress.

7.4 Influence of Residual Stress (Preapplied Stress) on Characterization of Plastic Zones

Figure 9 shows the influence of residual stress on the plastic zone. The plastic zone develops toward the area under the indenter when residual stress is compressive stress, and toward the opposite direction when residual stress is tensile stress, as shown in Fig. 9(a) and (b), respectively. Further research found that a larger tensile stress is associated with a larger plastic zone, and it is interesting that, by comparing the developing of the plastic zone between Fig. 9(a) and (c), the size of the plastic zone is seen to develop mainly along the indentation depth direction.

8. Conclusions

The experiment and finite element analysis were done for copper specimens by flat cylindrical indenters, and the following conclusions can be drawn:

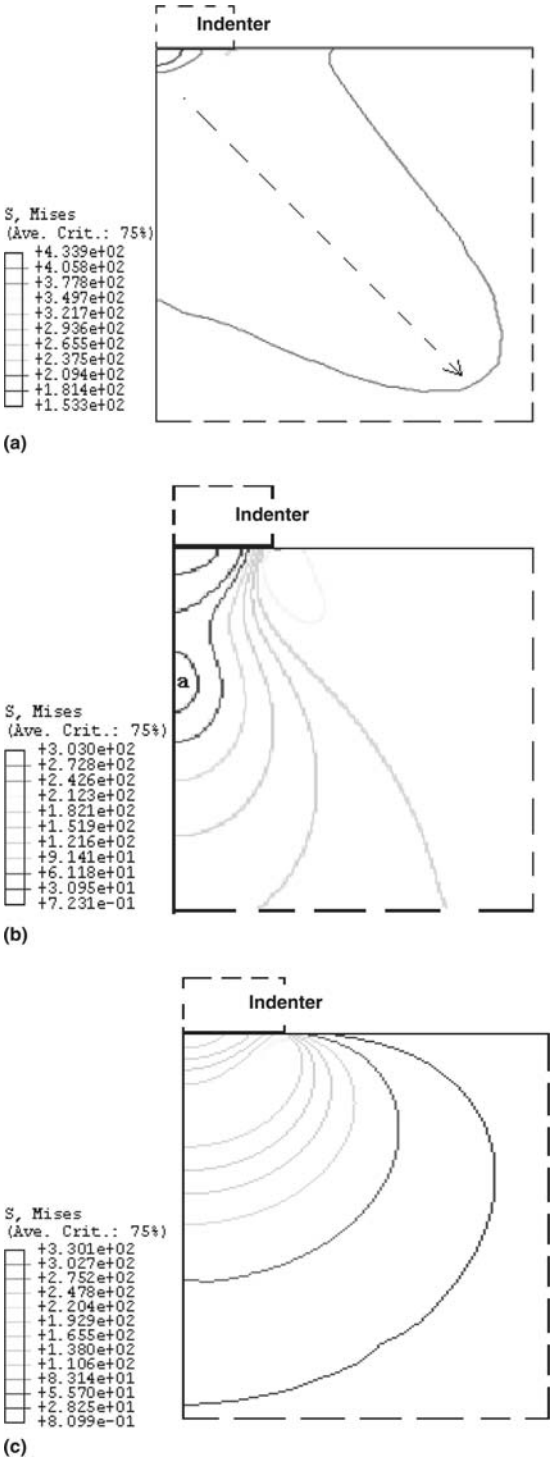

Fig. 8 Mises stress distribution ahead of the indenter with residual stress: (a) residual stress is compressive stress, 200 MPa; (b) residual stress is tensile stress, 200 MPa; (c) Mises stress distribution ahead of the indenter without residual stress

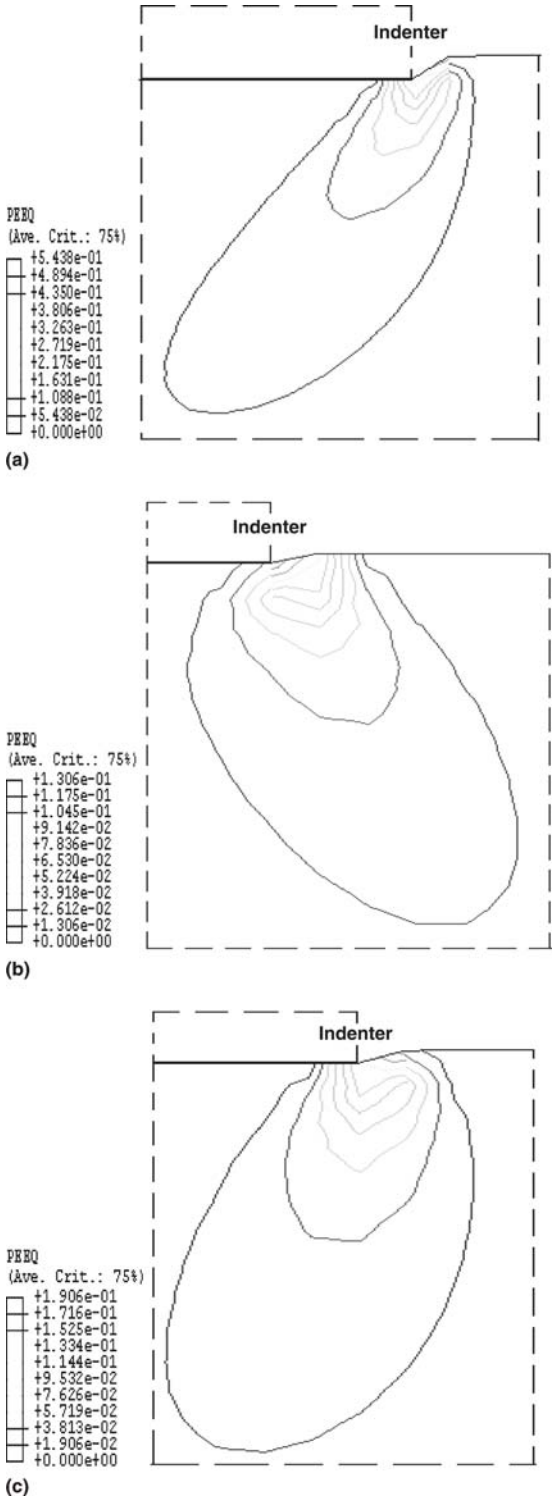

Fig. 9 Plastic zones developed for different residual stress: (a) residual stress is compressive stress, 200 MPa; (b) residual stress is tensile stress, 200 MPa; (c) plastic zones ahead of the indenter without residual stress

- The indentation experiment shows that the influence of anneal temperature on the loading-indentation depth curves are very larger in the "elastic-plastic transition region," which denotes that the influence of residual stress on the "elastic-plastic transition region" is also obvious.
- A method has been put forward to determine elastic modulus and Poisson ratio step-by-step with flat cylindrical indentation. Residual stress can also be determined if the yield strength is known in advance. This method avoids calculating contact area through the unloading curves and improves the experimental accuracy.
- Finite element analysis has also shown that the influence of residual stress on stress distribution ahead of the in-

denter is very large. Especially when residual stress is tensile stress, there exists another low stress, and it is the result that compressive stress induced by humps near the indentation interacts with residual tensile stress.

Acknowledgments

This work is supported by the National Nature Fund of China (10472094, 50375124), the Aviation Fund of China (03B53003, 02C53011), and the Graduate Starting Seed Fund of Northwestern Polytechnical University (Z200533).

References

1. M.F. Doerner and W.D. Nix, A Method for Interpreting the Data from Depth-Sensing Indentation Measurements, *J. Mater. Res.,* 1986, **4,** p 601-616
2. W.C. Oliver and G.M. Pharr, An Improved Technique for Determining Hardness and Elastic Modulus Using Load and Displacement Sensing Indentation Experiments, *J. Mater. Res.,* 1992, **7,** p 1564-1583
3. Z.F. Yue and G. Eggeler, Determination of Elastic and Creep Properties of Thin-Film Systems from Indentation Experiments, *J. Mater. Sci. Technol.,* 2000, **16,** p 559-567
4. J.N. Florando and D.W. Nix, Study of Yielding and Strain Hardening Behavior of a Copper Thin Film on a Silicon Substrate Using Microbeam Bending, *Mater. Res. Soc. Symp.,* 2001, **673,** p 191-196
5. J.L. Bucaille, S. Stauss, P. Schwaller, and J. Michler, A New Technique to Determine the Elastic-Plastic Properties of Thin Metallic Films Using Sharp Indenters, *Thin Solid Films,* 2004, **447,** p 239-245
6. Z.F. Yue and Z.Z. Lu, A Numerical Determination of the Fiber/Matrix Interlayer Creep Properties from the Indentation Creep Testing in Fiber Reinforced Composites, *Mater. Sci. Eng.,* 2003, **A352,** p 266-272
7. H. Chen and J.C.M. Li, Viscosity of an ABS Polymer Measured by Impression Test, *Micromechanics of Advanced Materials,* S.N.G. Chu et al., Ed., TMS, 1995, p 367-371
8. W. Sun and T.H. Hyde, A Potential Method for Determining the HAZ Properties in Welds Using Two Materials Impression Creep Test, *Acta Metall. Sin.,* 2004, **17,** p 591-596
9. Y. Huang, Z. Xue, H. Gao, W.D. Nix, and Z.C. Xia, A Study of Microindentation Hardness Tests by Mechanism-Based Strain Gradient Plasticity, *J. Mater. Res.,* 2000, **15**(8), p 1786-1796
10. X. Cai and H. Bangert, Hardness Measurements of Thin Films—Determining the Critical Ratio of Depth to Thickness Using FEM, *Thin Solid Films,* 1995, **264,** p 59-71
11. Y.-H. Yoo, W. Lee, and H. Shin, Effect of Work Hardening on the Critical Indentation Limit in Spherical Nano-Indentation of Thin Film/Substrate Systems, *Surf. Coat.,* 2004, **179,** p 324-332
12. B.X. Xu and Z.F. Yue, Determination of the Elastic-Plastic Parameters of Multi-layer Material Systems by the Indentation Method with Flat Cylindrical Indents, in press
13. R.M. Souzaa, G.G.W. Mustoeb, and J.J. Moorec, Finite Element Modeling of the Stresses, Fracture and Delamination during the Indentation of Hard Elastic Films on Elastic-Plastic Soft Substrates, *Thin Solid Films,* 2001, **392,** p 65-74
14. T.S. Byun, S.H. Kim, B.S. Lee, I.S. Kim, and J.H. Hong, Estimation of Fracture Toughness Transition Curves of RPV Steels from Ball Indentation and Tensile Test Data, *J. Nucl. Mater.,* 2000, **277,** p 263-273
15. G. Sines and R. Carlson, Hardness Measurement for Determination of Residual Stress, *Bull. Am. Soc. Test. Mater.,* 1952, **180,** p 35
16. T.Y. Tsui, W.C. Oliver, and G.M. Pharr, Influences of Stress on the Measurement of Mechanical Properties Using Nanoindentation: I. Experimental Studies in an Aluminum Alloy, *J. Mater. Res.,* 1996, **11,** p 752-759
17. A. Bolshakov, W.C. Oliver, and G.M. Pharr, Influences of Stress on the Measurement of Mechanical Properties Using Nanoindentation: II. Finite Element Simulations, *J. Mater. Res.,* 1996, **11,** p 760-768
18. S. Suresh and A.E. Giannakopoulos, A New Method for Estimating Residual Stresses by Instrumented Sharp Indentation, *Acta. Mater.,* 1998, **46,** p 5755-5767
19. J.G. Swadener, B. Taljat, and G.M. Pharr, Measurement of Residual Stress by Load and Depth Sensing Indentation with Spherical Indenters, *J. Mater. Res.,* 2001, **16,** p 2091-2102
20. B. Taljat and G.M. Pharr, Measurement of Residual Stresses by Load and Depth Sensing Spherical Indentation, *Thin Films: stress and mechanical Properties,* Vol VIII, R. Vinic, O. Kraft, N. Moody, and E. Shaffer III, Ed., Materials Research Society, 2000, p 519-524
21. C.M. Lepienski, G.M. Pharr, Y.J. Park, T.R. Watkins, A. Misra, and X. Zhang, Factors Limiting the Measurement of Residual Stresses in Thin Films by Nanoindentation, *Thin Solid Films,* 2004, **447-448,** p 251-257
22. M. Bai, K. Kato, N. Umehara, and Y. Miyake, Nanoindentation and FEM Study of the Effect of Internal Stress on Micro/Nano Mechanics Property of Thin CN*x* Films, *Thin Solid Film,* 2000, **377,** p 138-147
23. W.C. Hayes, L.M. Keer, G. Herrman, and L.F. Mockros, A method for theoretical analysis of articular cartilage, *J. Biomech.,* 1972, **5,** p 541-551
24. D. Tabor, *The Hardness of Metals*, Clarendon Press, Oxford, 1951
25. R.T. Shield, On the Plastic Flow of Metals Under Conditions of Axial Symmetry, *Proc. R. Soc. London,* 1955, **A233**, p 267-271
26. D. Dorothee, R. Klaus, S. Bridit, S. Bernhard, and E. Gunther, Creep of a TiAl Alloy: A Comparison of Indentation and Tensile Testing, *Mater. Sci. Eng.,* 2003, **A357,** p 346-354
27. B.X. Xu, J.S. Wan, B. Zhao, and Z.F. Yue, Numerical Study of Creep Damage Behavior of Thin Film/Substrate Systems Under Indentation, *Mater. Sci. Eng. Technol.,* 2005, **36**(2), p 75-79
28. Hibbitt, Karlsson, and Sorensen, Inc., *ABAQUS User's Manual* (M), version 6.2